

W-68
ОБЪЕДИНЕННЫЙ
ИНСТИТУТ
ЯДЕРНЫХ
ИССЛЕДОВАНИЙ

Дубна

*Nucl. Phys., 1967, v. A93,
N1, p. 133-144*



E- 2580

J. Wilczyński , V.V. Volkov

DIFFRACTION EFFECTS IN THE
PROTON TRANSFER REACTIONS

ЛАБОРАТОРИЯ ЯДЕРНЫХ РЕАКЦИЙ

1966

E- 2580

4058/3 up

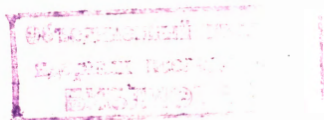
J. Wilczyński ^{x/}, V.V. Volkov

DIFFRACTION EFFECTS IN THE
PROTON TRANSFER REACTIONS

Submitted to Nuclear Physics

^{x/}

Jagellonian University, Cracow, Poland



1. Introduction

In a number of experiments on elastic and inelastic heavy ions scattering^{1-4/} the diffraction oscillations in angular distributions were observed when the values of the Coulomb parameter $\eta = mZ_1 Z_2 e^2 / \hbar^2 k$ were small. This indicates that in the interaction of heavy ions with nuclei the wave properties of particles are of importance.

One of the characteristic features of the interaction between complex nuclei is a strong absorption, connected with the compound nucleus channels. Therefore, the nuclear scattering radius is a well defined quantity, and thus one can compare the elastic scattering to the Fraunhofer diffraction by the "black disk". This analogy is rather good, provided that Coulomb distortions are small.

Another interesting case is single - or multi-nucleon transfer in the surface reactions. In contrast to elastic scattering, in transfer reactions no partial waves with large angular momentum l are present in the final reaction channel. This is due to the fact that as the distance between nuclei increases the probability of the transfer reaction is rapidly reduced. Thus, only several partial waves with angular momenta close to a certain value of l_0 , corresponding to a surface collision contribute to the reaction. This process is similar (from the viewpoint of the optical analogy) to the Fraunhofer diffraction by an annular aperture in a black screen. Therefore the diffraction effects in transfer reactions may also be expected.

The diffraction models of the transfer reactions have been recently developed by Frahn and Venter^{5/}, and Dar^{6/}. Occurrence of diffraction structure in angular distributions would be very essential for testing the validity of these models.

Our experiments were performed with the external C^{12} ion beam at the maximal energy of 82 MeV. The proton pick-up reaction (C^{12}, N^{13}) on two light nuclei C^{12} and Al^{27} was studied. As the value Z of the target nucleus is increased the conditions for detecting diffraction become worse due to the reduced oscillation period and the increase of the Coulomb interaction effect. The advantage of the chosen reaction (C^{12}, N^{13}) is that the reaction product N^{13} has no bound excited states, therefore it is possible to get information on the final target-nucleus excitation from the data on the N^{13} energy spectrum.

Besides, in pick-up reactions the final reaction channel is well defined, while in stripping reactions, besides the transfer mechanism, the mechanism of knocking free nucleons out of the projectile is also possible.

The N^{13} nucleus is a β^+ emitter with a 10 minute half-life. This property makes it very convenient for detecting.

2. EXPERIMENTAL PROCEDURE

2.1. Performance of Experiment

The experiments were performed at the 150 cm cyclotron of the Laboratory of Nuclear Reactions, JINR. The external C^{12} ion beam after being focused with two pairs of quadrupole lenses passed through a collimator and entered the reaction chamber (fig.1). The target was placed in the centre of the chamber or on the front wall, depending upon the angle region and the necessary angular resolution.

The radioactive products of transfer reactions emitted from the target were collected on the aluminium catcher foils placed on the internal surface of the chamber. After a 10 minute bombardment of the target the back flange of the reaction chamber was quickly removed, the catchers with activity were taken out, cut into circular rings corresponding to different angles of emission and put to the detector.

Besides N^{13} nuclei, other radioactive products were produced during the irradiation, causing a perturbing background. The main part of the background was due to C^{11} (β^+ , $T_{1/2} = 20$ min), produced in the neutron stripping reaction. In order to achieve the best conditions for detection of N^{13} , the difference between the N^{13} and C^{11} ranges was utilized. Due to smaller stopping power, the C^{11} ranges were larger and therefore one could find a layer in the catcher where mostly N^{13} nuclei stopped, while the C^{11} contribution was smaller. For each C^{12} incident energy such optimal layer was found experimentally by measuring the activity distribution in the aluminium foil stacks placed at different angles. To decrease the variation with the angle of the effective thickness of the catcher, a conic insert was used in the chamber which made it possible to place catchers in such a way that they were approximately perpendicular to the direction of the reaction product emission. For measuring the energy spectrum of N^{13} the foil stacks of aluminium foil, 0.4 mg/cm^2 thick were used.

After passing through the target the ion beam entered the Faraday cup connected with the electronic current integrator. To take into account the beam intensity fluctuations during the irradiation, the data from the integrator were

taken every minute. To avoid distortions due to electrons knocked by the beam out of the Faraday cup, of the target and of the edges of the diaphragms, electric magnets were placed in front and in the middle of the Faraday cup. The measurements showed that the influence of the knocked out electrons upon the current measurements was insignificant. The current measurements with the magnets switched on and off differed only by about 3%.

It turned out in practice that distortions in the current measurements could be due to the gas ionization by the beam if the vacuum near the Faraday cup is poor. Small size of diaphragm openings did not allow to reach the necessary vacuum in the chamber by diffusion pumping through the collimator. Therefore the tube of the Faraday cup was provided with an additional diffusion pump and a vacuum gauge to check the pressure.

The C^{12} energy was varied by inserting aluminium absorbers into the beam in front of the collimator. The energy losses and the effective ion charge after passing through the absorber were determined by using the data of Northcliff^{7/}.

2.2. Angular Resolution

Since the expected oscillation period equals only to several degrees, good angular resolution is a necessary condition for observing diffraction. In our experiment the angular resolution was determined by the distance from the target to the catchers, the width of the catcher rings, the diameter of the collimated beam and angular spread of particles in the beam. The cylindrical reaction chamber was 20 cm in diameter and 20 cm length. The catcher rings were usually 3 mm wide which corresponded to the angle range of about 0,8 degrees. The collimator diaphragm openings were 4 mm in diameter and were placed at 23 cm from each other. The angular spread of particles in the beam after collimating could be estimated by the diameter of a spot made on a sheet of paper which was placed on the back flange inside the chamber.

The average angular resolution was about one degree.

The reciprocal location of the chamber axis and the ion beam axis was of great importance. To provide their coincidence the sheet of paper fixed on the back flange inside the chamber was bombarded for a short time before each experiment. After obtaining the "picture" of the beam it was possible to adjust the position of the chamber with respect to the beam axis. The exactness of this adjustment was about 1 mm.

Small errors in determining $\Delta\theta$ were due to the procedure of cutting the catcher foils into narrow rings. The catchers were weighed after measurements to correct these errors.

2.3. Detecting Arrangement

The reaction products - N^{13} nuclei - were detected by counting the annihilation gammas produced from $N^{13} \beta^+$ decay. The schematic drawing of the arrangement is shown in fig.2. The detector consists of a system of two scintillation counters close to each other with NaI (Tl) crystals 80x 80 mm in size, connected to the coincidence circuit. After bombardment the aluminium catchers were put into copper molds 20x20x3 mm which were inserted into a slot between the crystals. The N^{13} decay positons stopped in the mold walls produced pairs of annihilation gammas detected by the circuit.

Pre-amplifiers, amplifiers and single-channel analyzers with a variable width of the gate were included in every branch of the circuit.

Usually, the amplification coefficient and the analyzer gate width were so chosen that they let through only the pulses associated with a "photopeak". To provide the simultaneity of the pulses applied to the coincidence circuit variable delayed lines were used. To reduce the background the detectors were shielded with lead, and a lead separator 8 mm thick was inserted between the crystals. There was a channel in the separator to place the molds with the catchers.

The efficiency of the arrangement was determined by use of the Na^{22} source. For this purpose the total efficiencies of the crystals for 511 keV gammas, for 1276 keV gammas and for coincidences of annihilation gammas were calculated. The beta-plus-intensity of the Na^{22} source was determined by measurements in operation conditions when the full gamma spectra were detected (single-channel analyzers were open).

The efficiency of the arrangement was 11% when only photopeak coincidences were registered, while the background was about 1 pulse per minute. The efficiency of the arrangement could be increased, when besides the photopeak the Compton part of the spectrum was also detected, although the background of the arrangement was thus increased.

3. RESULTS AND DISCUSSION

3.1. Energy Spectra of Reaction Products

The energy distribution of N^{13} products from the reactions $Al^{27}(C^{12}, N^{13})Mg^{26}$ and $C^{12}(C^{12}, N^{13})B^{11}$ are shown in figs. 3 and 4. These distributions were measured for the angle region where diffraction was observed and at energies close to those at which angular distributions were studied. The schemes of Mg^{26} and B^{11} levels are shown above the spectra. Insufficient resolution due to the energy spread in the beam and the limitations of the catcher foil method does not permit to distinguish the transitions to separate levels, however, the general picture of the spectrum, especially its half-width, are very significant for the analysis of diffraction structure.

Fig.3 shows that as aluminium is bombarded, in the Mg^{26} residual nucleus several levels, approximately up to 5.5 MeV are excited. The region of the observed excitations does not significantly change with energy, although the maximum of the distribution is displaced to the region of higher excitation with the increase of C^{12} energy.

In the reaction $C^{12}(C^{12}, N^{13})B^{11}$ the residual nucleus B^{11} remains mainly in the ground state or in the first excited state at 2.14 MeV. Similarly to the reaction on aluminium, the incident energy increase leads to the increase of the excited state contribution.

3.2. Angular Distributions

The angular distributions of N^{13} in the reactions $Al^{27}(C^{12}, N^{13})Mg^{26}$ and $C^{12}(C^{12}, N^{13})B^{11}$ obtained at several C^{12} energies are shown in figs. 5, 6 and 7. Experimental points referring to different sets of measurements are denoted by different signs. Errors due to statistical spread, uncertainty in decay curve analysis and uncertainty in the determination of angular widths of the catchers are less than 5%.

The results show that in the studied transfer reactions diffraction oscillations are rather distinct, especially in the low angle region. As the ion energy decreases and the Coulomb parameter η gets larger, oscillations are damped and the angular distribution is gradually transformed into the characteristic curve with the maximum corresponding to a surface collision of two nuclei.

Recently an attempt was made by Birnbaum^{8/} to detect diffraction in a single-nucleon transfer reactions when C^{12} target was bombarded with 148 MeV

N^{14} ions. The result appeared to be negative, no diffraction oscillations were found in the angular distributions. We believe that the negative result is due to limitations of the $(dE/dx) \times E$ method used in that work. By using this method it was very difficult to observe reaction products at low angles (the measurements were performed only at $\theta > 19^\circ$), however the diffraction structure is especially distinct at low angles.

We tried to analyse experimental data obtained in our work by means of the Frahn-Venter diffraction model. It should be noted that the present work was stimulated to a certain extent by the predictions of this model.

The diffraction model^{5/} considers the nucleon transfer reactions in quasi-elastic approximation. Frahn and Venter, considering transfer reactions as surface reactions and introducing a rather general dependence of the partial wave amplitudes upon the angular momentum l , obtained a comparatively simple analytical expression for the description of the reaction differential cross section. This expression includes equivalents for three quasi-classical parameters: R' is the interaction radius, d' is the effective width of the reaction region and r is the parameter associated with the strength of the transfer process. The model predicts diffraction oscillations proportional to the function $\sin(2T'\theta)$, where T' is the angular momentum parameter connected with the interaction radius. These oscillations modulate the smooth part of the differential cross section expression. The condition for damping of the diffraction oscillations is:

$$4\pi a(d'/R') \gg 1$$

The analysis of angular distributions made in terms of the Frahn-Venter model indicated that with the curves calculated on the basis of this model one cannot fit the experimental data. Trying to reach agreement in the positions of the maxima and minima one gets a large disagreement between the overall angular dependences and vice versa. The comparison between calculated curves and experimental data at the maximal energy is shown in fig. 8 (A and B).

In fig.8 (C and D) this comparison is made for the extreme case in which the Coulomb interaction is neglected. This case corresponds to the Kirchhoff formula for Fraunhofer diffraction by an annular aperture in a black screen: the angular dependence of the reaction amplitude is determined by the cylindrical Bessel function of order zero $-J_0(T'\theta)$. The main features of this classical dependence are present in the experimental angular distributions.

The disagreement between predictions of the Frahn-Venter model and experimental data is probably due to the fact that the authors take into account

only the Coulomb distortions of the incoming and outgoing waves. This is correct when the Coulomb parameter α is sufficiently large. Indeed, for the $\text{Al}^{27}(\text{C}^{12}, \text{N}^{13})\text{Mg}^{26}$ reaction at the C^{12} lowest energy (see fig. 6), for which $n = 6.88$, the Frahn-Venter curve fits quite well to the experimental data, giving a reasonable value of the r_0' parameter (1.54 fm).

Our results were also analyzed in terms of the Kalinkin-Grabowski model^{9,10/} in which methods of the optical model were used for the study of elastic scattering and transfer reactions. In this model the parameters connected with the real part of the Saxon-Wood nuclear potential and with the absorption were obtained from the analysis of the heavy ions elastic scattering data. The probability of transfer depends upon the α parameter related to the matrix element of the transition. In paper^{11/} this model was modified with a view of the account of diffraction effects. In fig. 5 solid lines denote the results obtained by the authors of this paper in case of the reaction $\text{Al}^{27}(\text{C}^{12}, \text{N}^{13})\text{Mg}^{26}$.

In the calculations the data were averaged over a certain angle interval $\Delta\theta$ associated with the angular resolution and with the energy spectrum of reaction products.

It is noteworthy that the width of the energy spectrum of reaction products is very significant for the distinctness of diffraction oscillations. The angular distribution in the neutron stripping reaction $\text{Al}^{27}(\text{C}^{12}, \text{C}^{11})$ at the energy 56.1 MeV is shown in fig. 9. The angular resolution in this experiment was the same as in the proton pick-up reaction, however, the energy spectra of reaction products were significantly different. In the reaction $(\text{C}^{12}, \text{C}^{11})$ the half-width of the energy spectrum is about 8 MeV. As a result, diffraction oscillations in the C^{11} angular distribution practically disappear. The curve from paper^{11/} given in this figure was calculated with the account of the C^{11} wide energy spectrum.

The comparison of the experimental data with the theoretical results from paper^{11/} indicates that the approach suggested by Kalinkin et al. is sufficiently general and permits to consider scattering and transfer reactions on the same basis.

The authors thank Professor G.N. Flerov, Corresponding Member of USSR Academy of Sciences, for permanent interest and useful discussions.

The authors are grateful to the team of the 150 cm cyclotron, headed by B. Zager for incessant operation of the machine, and to assistants I. Arefyev and A. Zolkin for help in measurements.

The authors express gratitude to F.Gareyev, J.Grabowski and B.N.Kalinkin for permission to quote the results of their calculations before publication.

R e f e r e n c e s

1. E.Newman, P.G.Roll and F.E.Steigert. Phys. Rev. 122 1842 (1961).
2. P.G.Roll, E.Newman and F.E.Steigert. Nucl. Phys. 29 544 (1962).
3. A.M.Smith and F.E.Steigert. Phys.Rev. 125, 988 (1962).
4. D.J.Williams and F.E.Steigert. Nucl. Phys. 30, 373 (1962).
5. W.E.Frahn and R.H.Venter. Nucl. Phys. 59, 651 (1964).
6. A.Dar. Nucl. Phys. 55 (1964) 305; Phys. Rev. 139, B1193 (1965).
7. L.C.Northcliffe. Phys.Rev., 120, 1744 (1960).
8. J.Birnbaum. Doctoral Dissertation, Yale University, 1965.
9. B.N.Kalinkin and J.Grabowski. Proceeding of the Third Conference on Reactions between Complex Nuclei, edited by A.Ghiorso, R.M.Diamont, and H.E.Conzett (University of California Press, Berkeley, 1963) p.129; Acta Phys. Polonica 24, 435 (1963).
10. J.Grabowski, B.N.Kalinkin and N.F.Markova. Nucl. Phys. 65, 294 (1965).
11. F.Gareyev, J.Grabowski, and B.N.Kalinkin, preprint JINR.

Received by Publishing Department
on February 15, 1966.

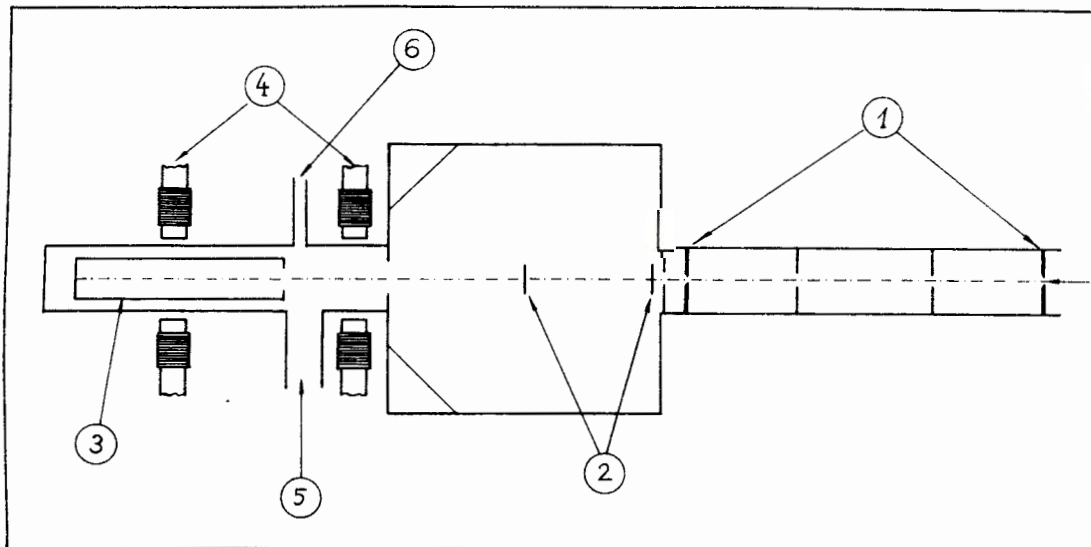


Fig. 1. Schematic drawing of the reaction chamber. 1. Collimator diaphragms, 2. Possible positions of the target, 3. Current collector, 4. Electric magnets, 5. Diffusion pumping, 6. Vacuum measurements.

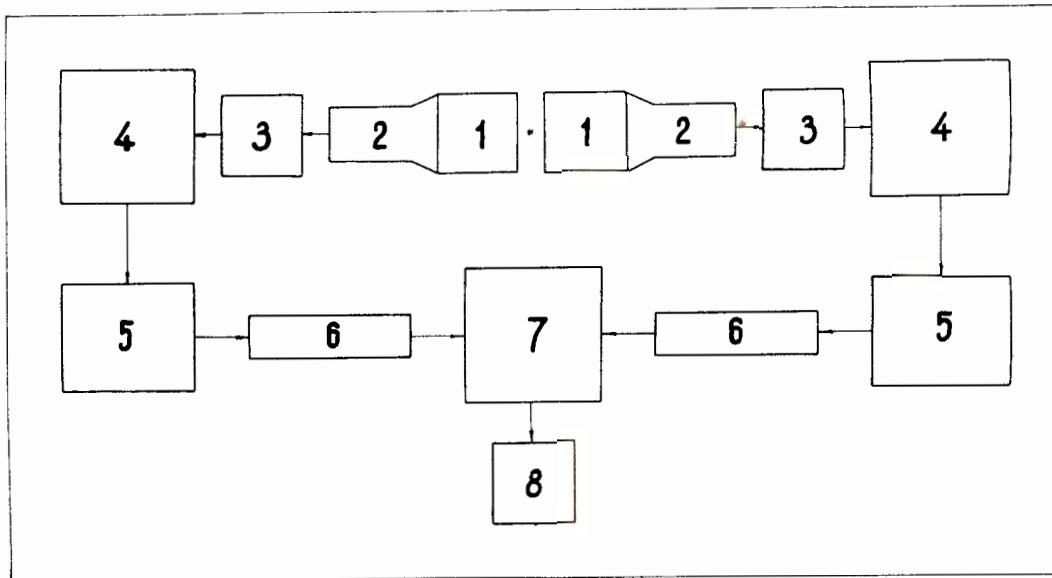


Fig. 2. Block diagram of the measuring arrangement. 1. NaI(Tl) crystals. 2. Photomultipliers FEU-24. 3. Pre-amplifiers. 4. Amplifiers. 5. Single-channel pulse analyzers. 6. Delayed lines. 7. Coincidence circuit. 8. Scaler.

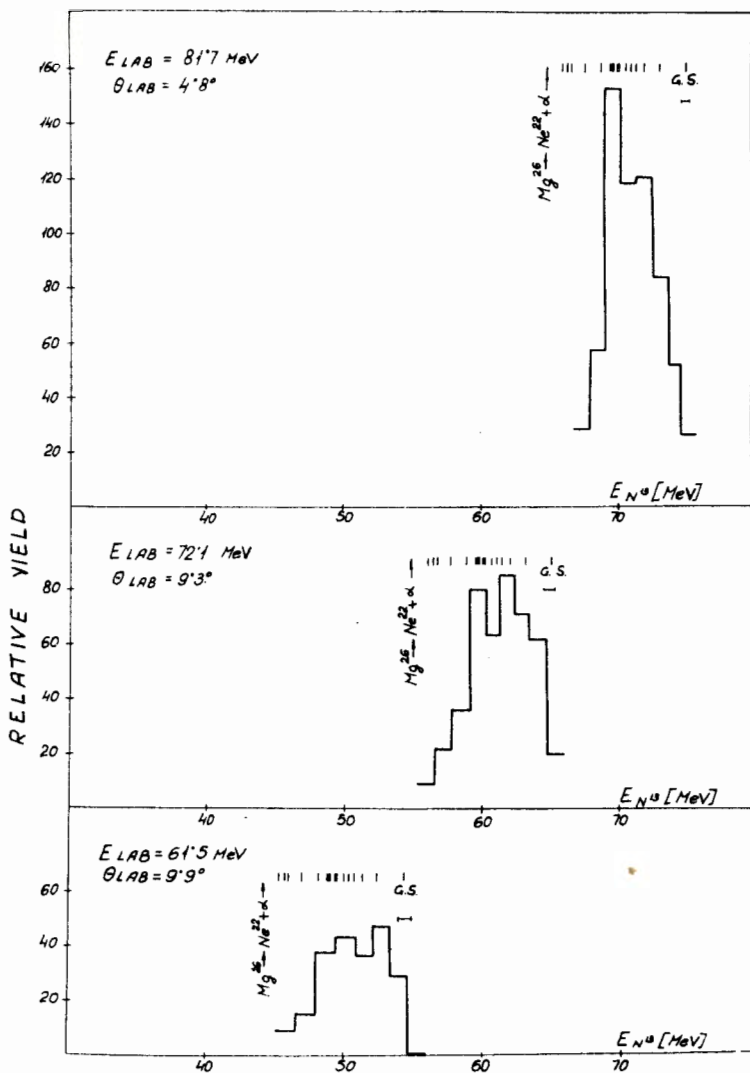


Fig. 3. Energy spectra of N^{13} products from the reaction $Al^{27}(C^{12}, N^{13})Mg^{26}$. The scheme of the known excited states of the Mg^{26} final nucleus is given above the spectra. The bar below the designation of the Mg^{26} ground state shows the energy equivalent of the target thickness.

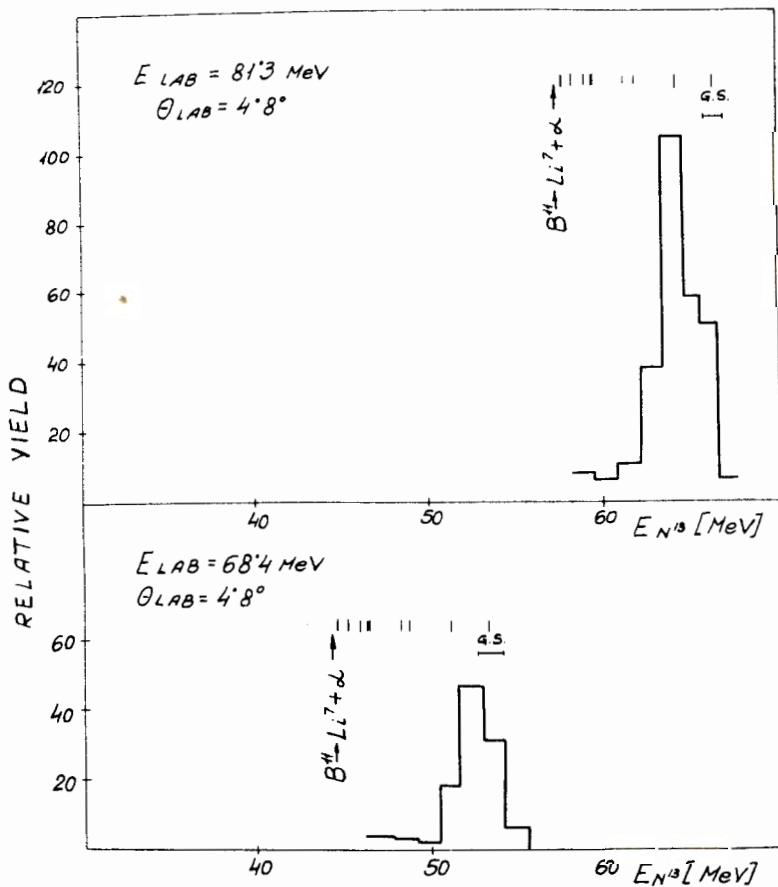


Fig.4. Energy spectra of N^{13} products from the reaction $C^{12}(C^{12}, N^{13})B^{11}$. The scheme of the known excited states of the B^{11} final nucleus is given above the spectra. The bar below the designation of the B^{11} ground state shows the energy equivalent of the target thickness.

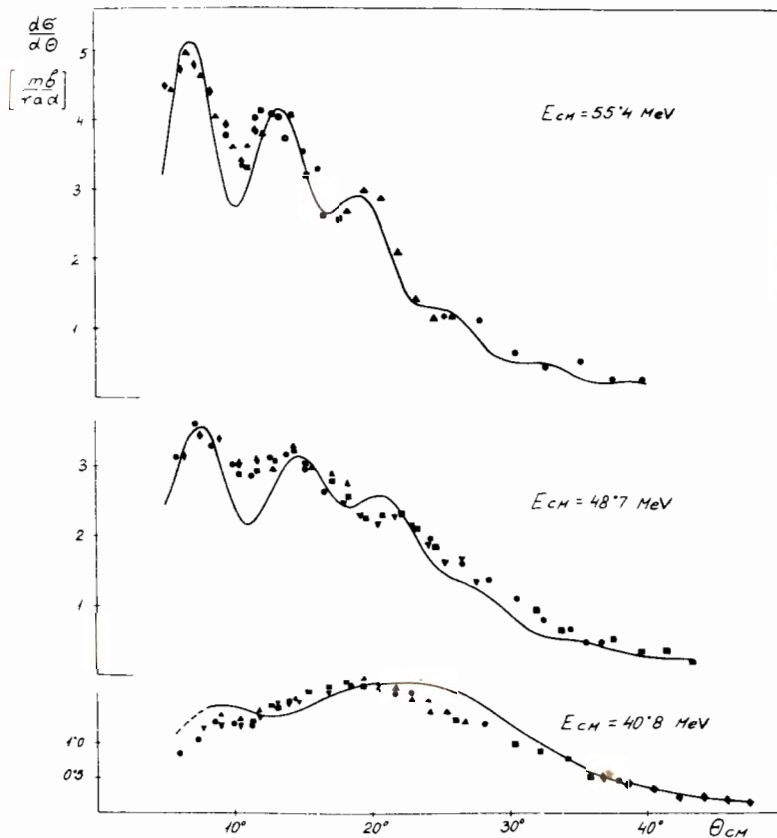


Fig. 5. Angular distributions in the reaction $Al^{27}(C^{12}, N^{13})Mg^{26}$. Different signs denote experimental points in different sets of measurement. Solid lines denote calculated curves of Gareyev, Grabowski and Kalinkin^{11/}.

$E = 55.4 \text{ MeV}$, $\alpha = 0.8 \text{ fm}^{-1}$, $\Delta\theta = 3.0^\circ$; $E = 48.7 \text{ MeV}$, $\alpha = 0.8 \text{ fm}^{-1}$, $\Delta\theta = 4.0^\circ$; $E = 40.8 \text{ MeV}$, $\alpha = 0.7 \text{ fm}^{-1}$, $\Delta\theta = 7.5^\circ$.

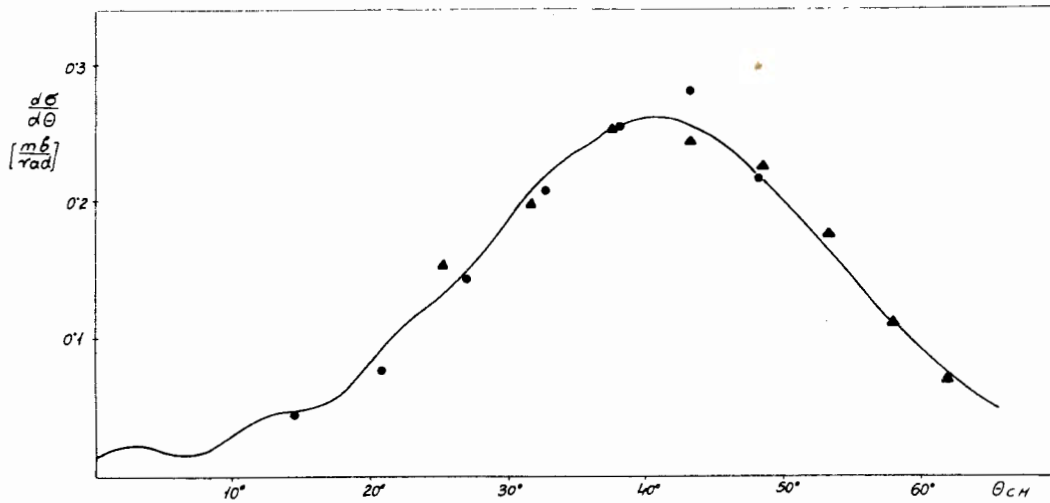


Fig. 6. Angular distribution in the reaction $\text{Al}^{27}(\text{C}^{12}, \text{N}^{13})\text{Mg}^{26}$ at $E = 26.4$ MeV ($n = 6.88$). The solid line is calculated on the basis of the Frahn-Venter model: $r'_0 = 1.54$ fm, $d' = 0.50$ fm, $r = 0.122$.

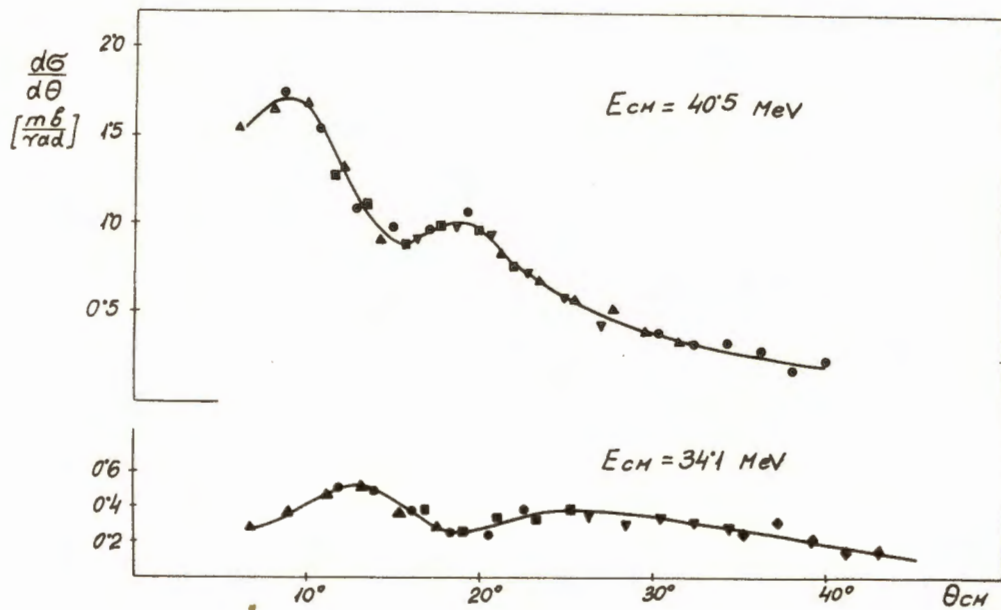


Fig. 7. Angular distributions in the reaction $C^{12}(C^{12}, N^{13})B^{11}$. Different signs denote experimental points in different sets of measurements.

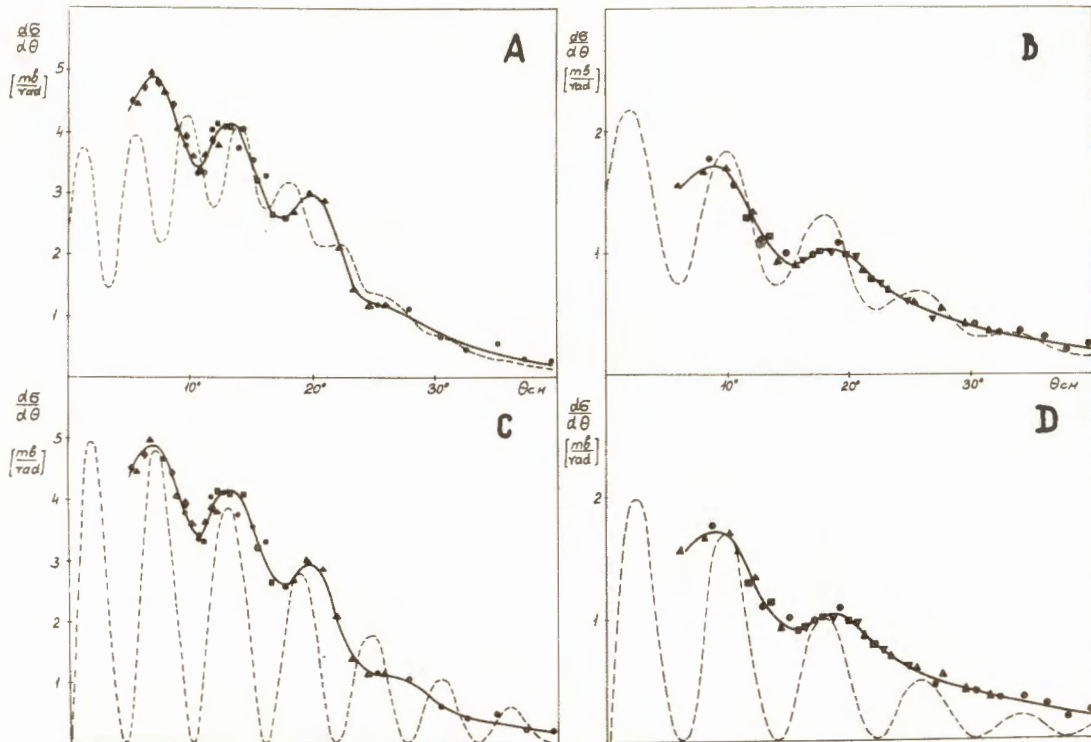


Fig. 8. A and C: Angular distribution in the reaction $\text{Al}(\text{C}^{12}, \text{N}^{18})\text{Mg}^{26}$ at $E=55.4$ MeV.
 B and D: Angular distribution in the reaction $\text{C}(\text{C}^{12}, \text{N}^{18})\text{B}^{11}$ at $E=40.5$ MeV. Solid lines are drawn through experimental points. Dashed curves are calculated on the basis of the Frahn-Venter model:
 A: $r'_0 = 1.88$ fm, $d' = 0.54$ fm, $r = 0.424$
 B: $r'_0 = 1.59$ fm, $d' = 0.51$ fm, $r = 0.228$.
 In figs. C and D dashed curves are calculated for the extreme case of the Frahn-Venter model where Coulomb interaction is neglected:
 C: $r'_0 = 1.45$ fm, $d' = 0.30$ fm. D: $r'_0 = 1.59$ fm, $d' = 0.48$ fm.

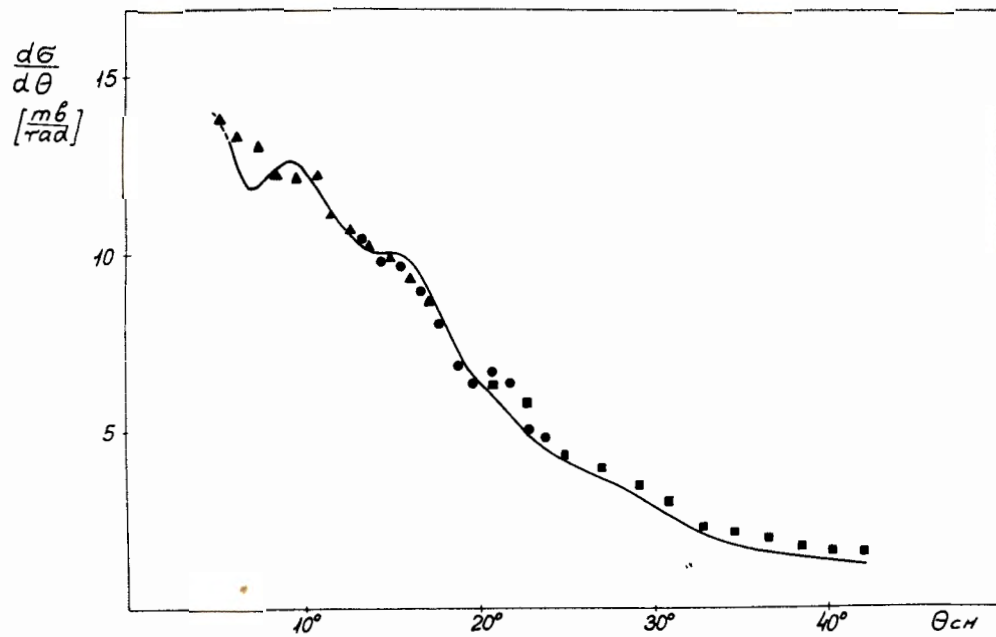


Fig. 9. Angular distribution in the neutron stripping reaction $\text{Al}^{27}(\text{C}^{12}, \text{C}^{11})$ at 56.1 MeV. The solid curve is calculated by Gareyev, Grabowski and Kalinkin¹¹: $a = 1.1 \text{ fm}^{-1}$, $\Delta\theta = 7^{\circ}20'$.